INDONESIAN JOURNAL ON GEOSCIENCE
Geological Agency
Ministry of Energy and Mineral Resources

Journal homepage: https://ijog.geologi.esdm.go.id
ISSN 2355-9314, e-ISSN 2355-9306

Petrology and Geochemistry of Ciremai Volcano, West Java, Indonesia: Evidence of Open-System Magma Dynamics

Keisha Prillia Qayyima[1], I Gusti Bagus Eddy Sucipta[2], Asep Saepuloh[2], Nurcahyo Indro Basuki[2], Very Susanto[2], Niniek Rina Herdianita[2], Mirzam Abdurrachman[2], Idham Andri Kurniawan[2], Prihadi Sumintadireja[2], and Emmy Suparka[2]

[1]Department of Geological Engineering, Bandung Institute of Technology, Bandung, Indonesia
[2]Petrology, Volcanology, and Geochemistry Research Group, Department of Geological Engineering, Bandung Institute of Technology, Bandung, Indonesia

Corresponding author: 22025002@mahasiswa.itb.ac.id
Manuscript received: March 03, 2025; revised: November 04, 2025;
approved: June 02, 2026; available online: October 21, 2026

Abstract - Ciremai Volcano is the youngest active volcanic system within the Ciremai Volcanic Complex (CVC), located on the northern coast of West Java. This study aims to further investigate the characteristics of the magmatic system as part of the Sunda Arc. The activity of the CVC is divided into four periods: Putri Volcano, Gegerhalang Volcano, Wurung Crater, and Ciremai Volcano with its parasitic cones. The magmatic evolution of the CVC is reflected in the characteristics of its lava throughout its volcanic history. Petrographic analysis reveals that the volcanic rocks of the CVC are predominantly composed of plagioclase, pyroxene, olivine, hornblende, and opaque minerals as phenocrysts. The magma exhibits calc-alkaline affinity, with Fe enrichment during the early stages of magma formation. The enrichment of incompatible elements (Sr, K, Rb, Ba, and Th), depletion of HFSE (Nb, P, and Ti), and the presence of xenoliths suggest a convergent margin setting, with a continental-derived sediment enrichment in the magmatic source. Both petrological and geochemical analyses indicate that the magmatic evolution of the CVC has an interconnected open-system magma dynamic. Major basaltic injections and mixing of basaltic magma likely triggered a significant eruption at the end of Gegerhalang and contributed to the development of new magma conduits. Besides fractional crystallization, the post-caldera magmatism of Wurung Crater, Ciremai, and its parasitic cones is affected by a prolonged basaltic influx and magma reheating.

Keywords: Ciremai Volcanic Complex (CVC), magmatic evolution, crustal contamination, open-system

© IJOG - 2026

How to cite this article:
Qayyima, K.P., Sucipta, I.G.B.E., Saepuloh, A., Basuki, N.I., Susanto, V., Herdianita, N.R., Abdurrachman, M., Kurniawan, I.A., Sumintadireja, P., and Suparka, E., 2026. Petrology and Geochemistry of Ciremai Volcano, West Java, Indonesia: Evidence of Open-System Magma Dynamics. *Indonesian Journal on Geoscience*, 13 (3), p.473-486. DOI:-0.17014/ ijog.13.3.473-486

Introduction

Background

The Ciremai Volcano is located in West Java, Indonesia (Figure 1), part of the Sunda Arc, which resulted from the convergence between the Indo-Australian Plate and the Eurasian Plate. This convergence is still ongoing up to today. Every tectonic process influences the formation of magmatic and volcanic processes, including those at Ciremai Volcano. Ciremai Volcano is a type A volcano (ESDM, 2021) with its most recent eruption recorded in 1951 (Stehn, 1940; Padang, 1951; Kusumadinata, 1971; Global Volcanism

PUBLISHED IN IJOG

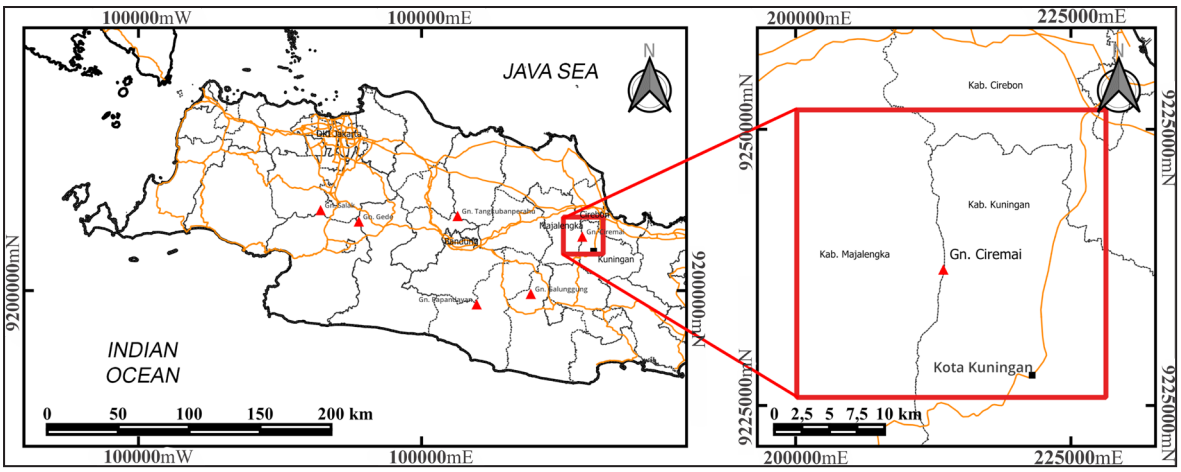


Figure 1. Location map of the studied area in the Ciremai Volcano, West Java, Indonesia, marked with the red box.

Program, 2025). The Ciremai Volcano occupies the rear-arc position, slightly apart from the main volcanic front of western Java.

Magmatic evolution in each volcano is key to unveiling the local magmatic behaviour and its relation to the regional scale. Changes in magmatic compositions, commonly affected by different basaltic magma influxes, clearly indicate an open magmatic system. Understanding magmatic compositions and evolution is significant for characterizing the tectonic setting, as well as predicting future eruptions and possible volcanic hazards. Many other type A volcanoes in the Sunda Arc have been the focus of numerous studies. In contrast, the Ciremai Volcano has received little attention, primarily due to its lower volcanic activity. Previous studies involving Ciremai have been conducted as a comparison of volcanoes in West Java (Sendjaja *et al*., 2009; Sendjaja and Kimura, 2010) or the Sunda Arc (Edwards, 1990; Dempsey, 2013). Despite its significance, detailed magmatic evolution of the Ciremai Volcano remains unexplored. Therefore, this study aims to investigate the magmatic source and evolution of the system in the Ciremai Volcanic Complex and its relationship with the tectonic setting to characterize potential eruptions in the future.

Geology of The Ciremai Volcano

The Ciremai Volcano is situated in the western Java region of the Sunda Arc. Given its position slightly isolated, northward from the main volcanic range in the area, Ciremai Volcano is regarded as part of a rear-arc region, with the Wadati-Benioff Zone at an approximate depth of 200 km (Sendjaja *et al*., 2009). The tectonic block beneath western Java is thought to be the South West Borneo (SWB) Block, which originated as a fragment of Australia. Along with the Argo and Inner Banda (IB) Blocks, the SWB Block detached from Australia in the Late Jurassic and accreted to Sundaland during the Cretaceous (Hall and Sevastjanova, 2012; Hall, 2014; Hall, 2017).

Ciremai Volcano lies on the top of some Tertiary sedimentary formations, such as Cinambo Fm., Kaliwangu Fm., Halang Fm., Ciherang Fm., Kalibiuk Fm., and Citalang Fm., some of which are intruded by an andesitic intrusion. The activity of the Ciremai Volcanic Complex (CVC) is divided into four periods, each with different volcanic centres. From the oldest, since the Pleistocene, there are the Putri Volcano, Gegerhalang Volcano, Wurung Crater, and the current Ciremai Volcano with its parasitic volcanoes (Figure 2; Djuri, 1973; Situmorang *et al*., 1995). The activity of the Gegerhalang Volcano ended with the formation of the Gegerhalang Caldera (Kadarsetia, 2013). The CVC is located in a densely structured area, trending northwest-southeast. The regional Pamanukan-Cilacap Fault Zone is associated with the primary geo-

PUBLISHED IN IJOG

logical structures in the.studied area The fault zone formed weak zones, serving as pathways for magma to move to the surface, thus controlling the formation and shifting of each magma conduit during each period. The geometry of the Gegerhalang Caldera is also influenced by the northwest - southeast trending structure.

Method and Materials

Geomorphological analysis and the geological map of the CVC modifications were based on field observations integrated with satellite imagery. Digital Elevation Model (DEM), Landsat-8, and Advanced Spaceborne Thermal Emission and Reflection Radiometer (ASTER) imagery were utilized to delineate geomorphological and lithological units, with fieldwork including sample collection. Modifications of the volcanostratigraphy of The CVC are based on the various hue, tone, surficial texture, and cross-cutting relationships observed from multiple satellite imageries, supported by field observations. Each sample obtained for this study represents a distinct lava unit from the magmatic history of the CVC (Figure 2).

This study is based on detailed petrographic and geochemical analyses of twenty-two volcanic rock samples representing eleven lava units and volcanic periods throughout the history of the CVC. Microscopic petrography, focusing on mineralogy, microtextures, and microstructures (Williams *et al*., 1982; Streck, 2008), was used to interpret magmatic processes and evolution within the complex. Fourteen representative samples, free of alteration and secondary minerals, were subsequently selected for the whole-rock geochemical analysis at P.T. Intertek Utama Services. Major, trace, and rare-earth elements were obtained using X-Ray Fluorescence (XRF) and Inductively Coupled Plasma - Optical Emission Spectroscopy/Mass Spectrometry (ICP-OES/MS). Major element (reported as oxides) analysis employed lithium metaborate fusion followed by XRF, with detection limits of 0.01 % for SiO_2, Al_2O_3, CaO, Cr_2O_3, Fe_2O_3(T), K_2O, MgO, MnO, Na_2O, and TiO_2, and 0.002 % for P_2O_5. For ICP-OES/MS, samples were digested using four acids (HCl, $HClO_4$, HNO_3, and HF) in teflon tubes, providing detection limits of 0.05

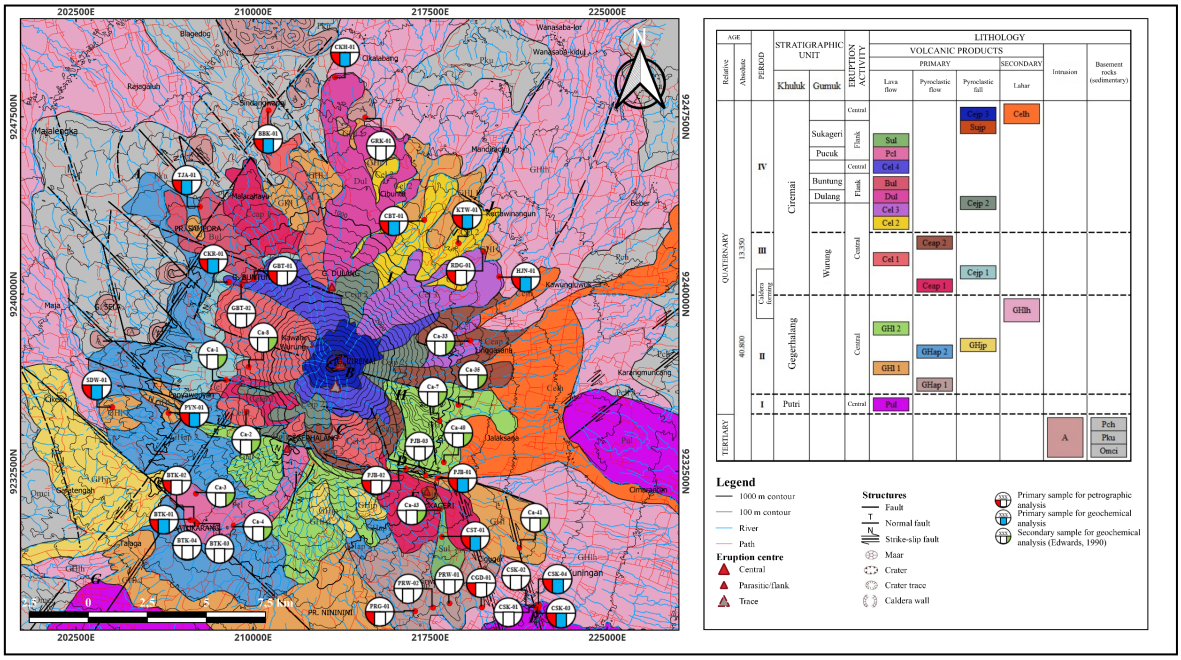


Figure 2. Geological map, volcanostratigraphy, and sampling locations of the Ciremai Volcanic Complex (Modified from Situmorang *et al*., 1995).

PUBLISHED IN IJOG

to 1 ppm for trace and rare-earth elements. Low Loss of Ignition (LOI) values (<0.01 to 0.65 %) indicate minimal weathering or alteration, ensuring that the geochemical data accurately reflect the magma composition.

Within the fourteen selected samples, two samples represent Putri, three represent Gegerhalang, one represents Wurung Crater, and eight represent Ciremai with its parasitic vents. The primary whole-rock geochemical data used herein is listed in Table 1. These primary data were compared with previous datasets (Edwards, 1990; Sendjaja *et al*., 2009; Al Rasyid, 2016) to characterize the magmatic source, processes, and evolutionary pathways, complementary to the petrographic evidence.

Result and Analysis

Petrological Analysis

Each period of activity formed bodies of lava flows, each with distinctive structures, which were observed in the outcrops (Figure 3), as well as different microscopic signatures. Most lava flow outcrops display a porphyritic texture, although a few exhibit an aphanitic texture. Lava flows from the Putri Volcano (first period) show some vertical joints and N190°E-trending brecciation. Lavas from the Gegerhalang Volcano (second period) exhibit an autobrecciated structure at its base, a massive structure in the middle, and sheeting joints (N102°E/17°SE) at the uppermost part. Lava bodies from the Wurung

Tabel 1. Whole-rock geochemical compositions from XRF and ICP-OES/MS analyses of primary samples of the volcanic rocks from the Ciremai Volcanic Complex.

Rock unit (After Situmorang *et al*.. 1995)	**Putri Volcano**		**Gegerhalang Volcano**			**Ciremai**
	Putri Lava (Pul)		**Gegerhalang Lava 1 (GHl 1)**		**Gegerhalang Lava 2 (GHl 2)**	**Ciremai Lava 1 (Cel 1)**
Eruptive period	**Period I**		**Period II**			**Period III**
Sample No.	**CSK-03**	**CSK-04**	**PYN-01**	**SDW-01**	**PJB-01**	**BBK-01**
Major elements (wt. %):						
SiO_2	54.87	55.37	56.53	54.85	53.45	58.21
TiO_2	0.83	0.81	0.70	0.92	0.83	0.71
Al_2O_3	19.01	19.09	17.30	18.18	19.73	17.44
Fe_2O_3	8.54	8.50	7.56	8.47	9.31	7.34
MnO	0.14	0.13	0.14	0.16	0.19	0.14
MgO	3.08	2.83	5.26	4.25	3.46	3.80
CaO	8.22	7.94	7.26	8.22	8.60	7.07
K_2O	1.31	1.36	1.50	1.53	1.00	1.80
Na_2O	3.32	3.37	2.98	3.14	3.01	3.13
P_2O_5	0.26	0.27	0.20	0.23	0.33	0.20
LOI	0.42	0.43	0.65	0.02	0.03	0.30
Total	**100.00**	**100.10**	**100.09**	**99.97**	**99.94**	**100.14**
Trace and Rare-Earth Elements (ppm):						
Rb	38.7	43.4	52.3	47.4	26.2	59.7
Sr	415	411	364	364	405	306
Y	23	20.9	18.8	22.6	20.8	20.7
Zr	121	124	131	134	98.2	147
Nb	5	5.2	5.9	5.9	4.6	5.9
Ba	263	260	313	299	225	314
La	16.4	16.4	18.1	17.4	15.3	17.5
Th	5.06	5.23	7.52	6.23	4.18	7.74
Ce	33.1	32.9	36.1	35	31.5	35.2
Nd	17.6	17.6	17.3	18.9	17.6	17.2
Sm	3.9	3.9	3.7	4.3	3.8	3.7
Gd	4.2	3.9	3.7	4.4	4	3.8
Tb	0.7	0.6	0.6	0.7	0.6	0.6
Yb	2.5	2.1	2	2.4	2.2	2.2
Lu	0.4	0.3	0.3	0.4	0.3	0.3
Hf	3.1	3.2	3.4	3.5	2.6	3.8
Ta	0.31	0.32	0.41	0.36	0.27	0.38

PUBLISHED IN IJOG

Table 1. Continued ...

Rock unit (After Situmorang *et al.*, 1995)	Ciremai Volcano (central eruption)				Ciremai Volcano (flank eruption)			
	Ciremai Lava 2 (Cel 2)		Ciremai Lava 3 (Cel 3)	Ciremai Lava 4 (Cel 4)	Buntung Lava (Bul)	Dulang Lava (Dul)	Pucuk Lava (Pcl)	Sukageri Lava (Sul)
Eruptive period	Period IV							
Sample No.	KTW-01	CBT-01	HJN-01	CKR-01	TJA-01	CKH-01	BTK-01	CST-01
Major elements (wt. %):								
SiO_2	56.45	58.55	54.85	56.61	59.35	54.71	57.24	54.81
TiO_2	0.68	0.68	0.85	0.75	0.70	0.78	0.78	0.84
Al_2O_3	16.49	17.12	18.51	16.78	17.45	16.56	17.43	17.21
Fe_2O_3	7.60	7.03	8.50	7.84	7.02	8.36	7.78	8.36
MnO	0.14	0.13	0.16	0.15	0.14	0.15	0.14	0.15
MgO	6.15	4.41	4.25	5.45	3.16	6.90	4.10	5.67
CaO	7.49	6.89	8.22	7.50	6.73	8.11	7.34	8.32
K_2O	1.74	1.73	1.32	1.68	1.99	1.45	1.80	1.48
Na_2O	2.85	3.08	2.97	2.96	3.30	2.74	3.19	2.86
P_2O_5	0.19	0.17	0.20	0.21	0.21	0.17	0.20	0.18
LOI	0.27	0.28	0.19	0.06	0.09	0.05	<0.01	0.07
Total	**100.06**	**100.08**	**100.02**	**99.99**	**100.13**	**99.98**	**100.00**	**99.95**
Trace and Rare-Earth Elements (ppm):								
Rb	57.8	60.3	41.4	57.8	70	49.4	60.1	48
Sr	329	318	320	311	325	287	298	289
Y	18.1	17.6	19.3	20.9	22.3	20.3	22.3	20.5
Zr	113	110	109	143	166	125	153	125
Nb	5.8	5.6	4.8	6.2	6.9	5.2	6.2	5.4
Ba	320	337	236	310	371	262	325	259
La	17	17.3	13.7	17.4	20	15.1	18	14.4
Th	7.58	7.73	5.52	7.5	9.21	6.25	8.06	6.1
Ce	33.4	34	28.2	35.4	40	30.4	35.9	29.5
Nd	15.6	15.6	14.9	17.6	19	15.6	18	15.6
Sm	3.4	3.3	3.4	3.9	4.1	3.6	4	3.6
Gd	3.4	3.2	3.7	3.9	4.1	3.8	4.1	3.8
Tb	0.5	0.5	0.6	0.6	0.7	0.6	0.7	0.6
Yb	1.8	1.9	2.1	2.2	2.4	2.1	2.3	2.1
Lu	0.3	0.3	0.3	0.3	0.4	0.3	0.4	0.3
Hf	3	2.9	2.8	3.6	4.3	3.2	3.9	3.2
Ta	0.39	0.39	0.31	0.42	0.47	0.34	0.42	0.34

Crater (third period) are generally structureless or massive. Most of the lava outcrops from Ciremai Volcano (and its parasitic volcanoes) display a sequence that includes autobreccia, massive lava, and sheeting joints, either present or absent, towards the top of the lava flow. Generally, the orientation of sheeting joints shows the eruption centre from which they originated.

Microscopic analysis shows that the petrological and mineralogical characteristics of the volcanic rocks throughout the activity of the CVC are varied, ranging from olivine basalts, basalts, pyroxene andesites, and hornblende andesites, based on textural characteristics from Williams *et al.* (1982) classification (Figure 4). All volcanic rocks showed a porphyritic texture, dominated by phenocrysts of plagioclase, clinopyroxene, orthopyroxene, olivine, hornblende, and some opaque minerals. In general, the plagioclase content within all products of the CVC is oligoclase-labradorite. An intersertal texture is observed in the groundmass of olivine basalts and basalts.

PUBLISHED IN IJOG



Figure 3. Photographs of outcrops in the CVC, showcasing distinctive structures. (a) Brecciated lava flow in Pul, (b) lava with (bottom to top) autobreccia, massive structure, and sheeting joints in GHl 2, (c) lava with (bottom to top) autobreccia and massive structure in Cel 3, (d) lava dome (Mount Buntung) in Bul, (e) lava with (bottom to top) autobreccia and massive structure in Dul, (f) lava with (bottom to top) autobreccia, massive structure, and sheeting joints in Pcl.

Period I (Putri Volcano, Pleistocene)

Lava flows from the activity of Putri Volcano (Pul) are found in the southwest, southeast, and eastern areas of the studied area. Based on microscopic analysis, the lava flows are classified as basalt, characterized by a distinctive intersertal texture. Microphenocrysts of orthopyroxene are commonly rimmed by clinopyroxene (Figure 4a). Some minerals are being altered into iddingsite, chlorite, and iron oxides.

Period II (Gegerhalang Volcano, Pleistocene)

The studied area contains products from the activity of the Gegerhalang Volcano.The first product of this period is a pyroclastic flow (GHap 1) with various fragments of volcanic rocks. One fragment is basalt (similar to basalt observed in the first period); another is hornblende andesite. The first lava unit in this period (GHl 1) are olivine basalt and basalt, with a microgabbro xenolith (Figure 4b). The last lava units (GHl 2) are hornblende andesites and basalts. Within the hornblende andesite, some hornblende phenocrysts have rims of fine-grained clinopyroxene and plagioclase, showing a disequilibrium texture (Figure 4c). Meanwhile, the basalt contains traces of hornblende, clinopyroxene phenocrysts rimmed by fine-grained orthopyroxene and a microgabbro xenolith.

Period III (Wurung Crater, Pleistocene - Holocene)

Lava from the Wurung Crater (Cel 1) generally flowed to the west, south, and north relative to the crater, also filling the Gegerhalang Caldera. Microscopically, this period comprised basalts, as shown by their signature intersertal texture in their groundmass. Within this unit, some large olivine crystals appear to have reaction rims of opaque minerals and orthopyroxene with symplectic intergrowth, hypothesized as antecrysts (Figure 4d). Antecrysts are foreign crystals within an igneous body, derived from an older and cogenetic magma (Tsuchiyama, 1986; Streck, 2008; Vernon, 2018).

Period IV (Ciremai Volcano, Holocene)

Products of this period originated from the main conduit of the Ciremai Crater (Cel 2, Cel 3, and Cel 4) and four parasitic volcanoes around the edifice of the Ciremai Volcano. The para-

PUBLISHED IN IJOG

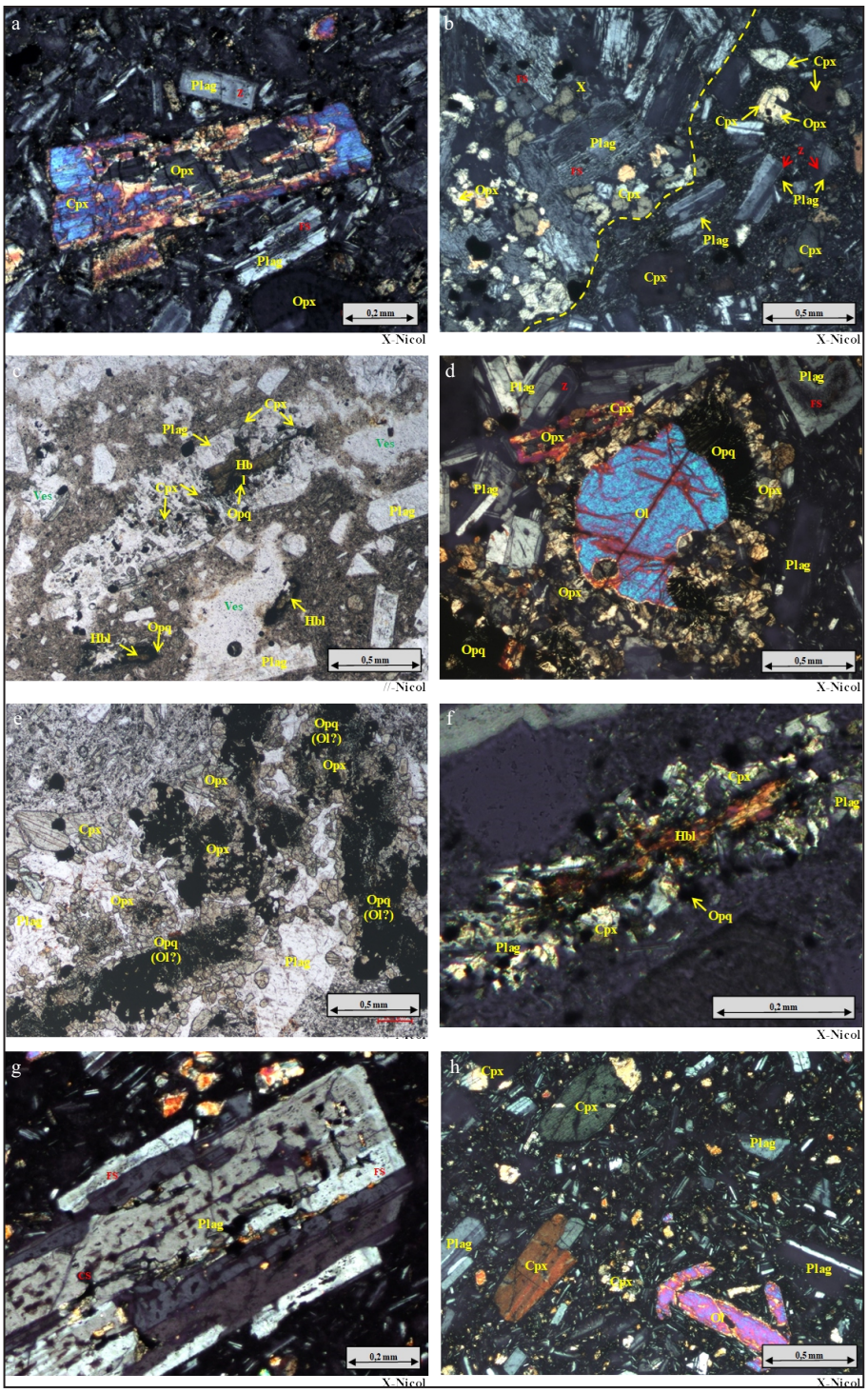


Figure 4. Photomicrographs of the volcanic rocks from the CVC, showcasing distinctive microtextures. (a) Orthopyroxene rimmed by clinopyroxene in Pul, (b) xenolith of microgabbro in GHl 1, (c) hornblende with a disequilibrium texture in GHl 2, (d) olivine antecrysts in Cel 1, (e) traces of olivine antecrysts in Cel 2, (f) hornblende with a disequilibrium texture in Bul, (g) coarse-sieved plagioclase in Pcl, and (h) skeletal olivine in Sul.

sitic volcanoes are Mount Dulang (Dul), Mount Buntung (Bul), Mount Pucuk (Pcl), and Mount Sukageri (Sul). Lava flows from this period are olivine basalts, basalts, and pyroxene andesites.

In lavas from the main crater, some plagioclase phenocrysts have sieve, zoning, resorption surface, and broken crystal microtextures (Renjith, 2014 classification). The oldest lava from the

PUBLISHED IN IJOG

main crater in this period (Cel 2) showed traces of olivine antecrysts (Figure 4e), despite the olivine core being fully altered into an opaque mineral. Whereas the lavas from the parasitic volcanoes are abundant in olivine, often showing plagioclase microtextures similar to those observed in other products in this period. Other distinct microtextures such as hornblende with disequilibrium texture (Bul; Figure 4f), coarse sieved plagioclase (Pcl; Figure 4g), and skeletal olivine (Sul; Figure 4h) were found.

Geochemical Analysis

Geochemical analysis was used to determine the origin and processes that occurred during the magmatic evolution. The whole-rock geochemistry data is presented in Table 1.

Magma Composition

Geochemical analysis was used to determine the origin and processes that happened during the magmatic evolution. Composition-wise, based on the Total Alkali ($Na_2O + K_2O$) vs. Silica (SiO_2) diagram (TAS Diagram, Le Bas *et al*., 1986; Figure 5a), lavas throughout the activity of each period in the CVC are basalts - andesites, with silica content ranging from 49.43 to 59.35 wt. %. All of the volcanic rocks fall under the sub-alkaline series.

Magma Affinity

Magmatic affinity using the K_2O vs. SiO_2 diagram (Peccerillo and Taylor, 1976; Figure 5b) showed that the samples have calc-alkaline affinity. A singular trend between K_2O against SiO_2 suggests the differentiation of a cogenetic magma. Further affinity identification using FeO*/MgO *vs*. SiO_2 diagram (Miyashiro, 1975; Figure 5c) and the AFM ternary diagram (Irvine and Baragar, 1971; Figure 5d) shows that the magma has calc-alkaline affinity, with an Fe enrichment during the early magma generation.

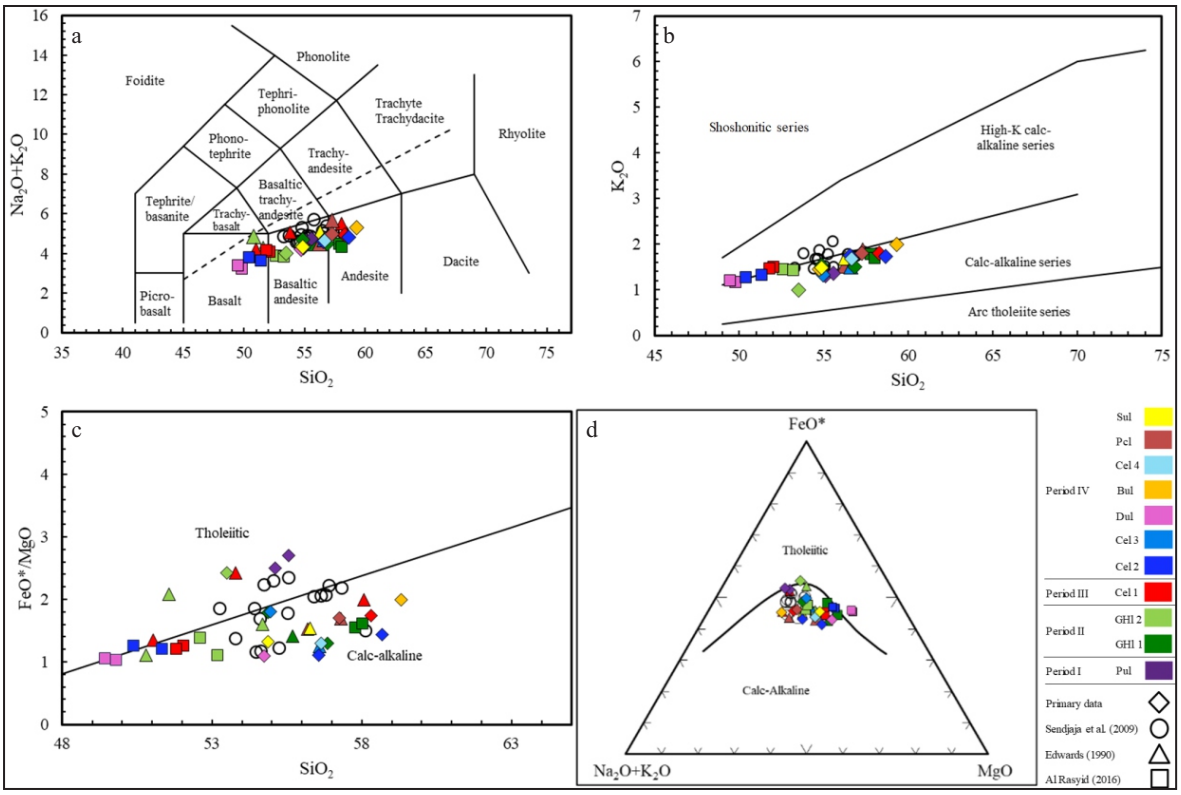


Figure 5. Classifications of magma chemical composition based on its (a) total alkali-silica (TAS; Le Bas *et al*., 1986) and magmatic affinity based on (b) K_2O *vs*. SiO_2 (modified from Peccerillo and Taylor, 1976), (c) FeO*/MgO *vs*. SiO_2 (Miyashiro, 1975), and (d) AFM Diagram (Irvine and Baragar, 1971).

PUBLISHED IN IJOG

Magma Differentiation (Major Elements)

Major elements as oxides are plotted against SiO_2 in the Harker Diagram (Figure 6). TiO_2, Fe_2O_3, and MgO display negative correlations with SiO_2 (Figure 6a-c), whereas Na_2O displays a positive correlation with SiO_2 (Figure 6d), all with a steeper slope gradient at lower SiO_2 content. On the other hand, CaO showed a slight increase with increasing SiO_2 at lower concentrations, followed by a decrease as SiO_2 continued to increase (Figure 6e). Higher concentrations of CaO at low SiO_2 are indicative of a Ca-rich pyroxene phase in the magma. Negative correlation between CaO and SiO_2 and positive correlation between Na_2O and SiO_2 indicate fractional crystallization of Ca-rich plagioclase to Na-rich plagioclase. The steeper slope gradient within some oxides suggests a more intense fractional crystallization of pyroxenes and/or olivines along with Fe-Ti oxides.

Trace and Rare EarthA Elements (REE)

Trace and rare-earth elements (REE) are more sensitive in determining magmatic source and tectonic setting. Enriched MORB (E-MORB) normalized (Sun and McDonough, 1989) trace and rare-earth elements (Figure 7a) display selective enrichment in Large Ion Lithophile Elements (LILE; Rb, Ba, Th, and K) and depletion of High Field Strength Elements (HFSE; Nb, P, and Ti), accompanied by the slope of Light-REE (LREE) gradually flattening towards Heavy-REE (HREE). Based on the relative abundance, the magma forming the CVC resulted from the melting of oceanic crust, associated with a convergent margin.

Selected trace elements from Ciremai were compared with an island arc and an active continental arc, consecutively the Tonga-Kermadec Arc and the Andes Arc. Figure 7b). Normalized to MORB (Pearce, 1983), volcanic rocks from Ciremai show selective enrichment in incompatible elements (Sr, K, Rb, Ba, and Th) with lower Ta and Nb. The relative abundance from CVC displays more similarities to the Andes Arc. An enrichment of Th relative to Ba is indicative of upper-crustal contamination (Rudnick and Gao, 2014). The singular evolutionary trend and relatively homogeneous concentrations of trace and rare-earth elements in the volcanic rocks of the CVC suggest similar processes in an interconnected magmatic system throughout the CVC history.

In determining between tectonic settings, ratios of Zr/Y vs. Zr (Pearce, 1983), Th/Nb vs. La/Yb, and Nb/La vs. La/Yb (Hollocher *et al.*, 2012) (Figures 8a−c) show that the volcanic system formed in a continental arc. Processes within its magmatism, which is also influenced

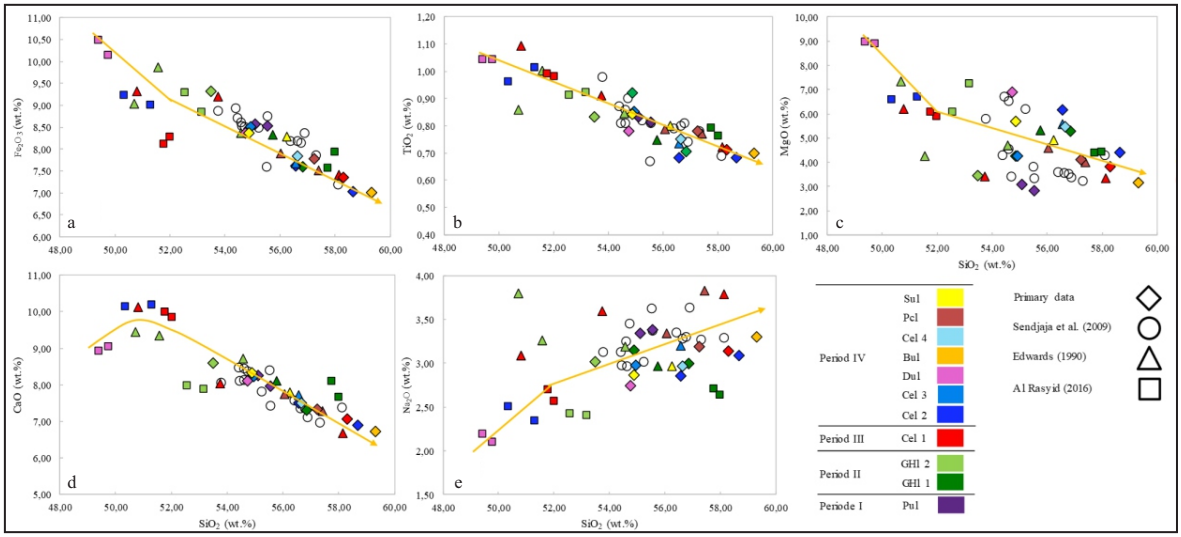


Figure 6. Harker variation diagram of (a) Fe_2O_3, (b) TiO_2, (c) MgO, (d) CaO, and (e) Na_2O, against the differentiation index of SiO_2.

PUBLISHED IN IJOG

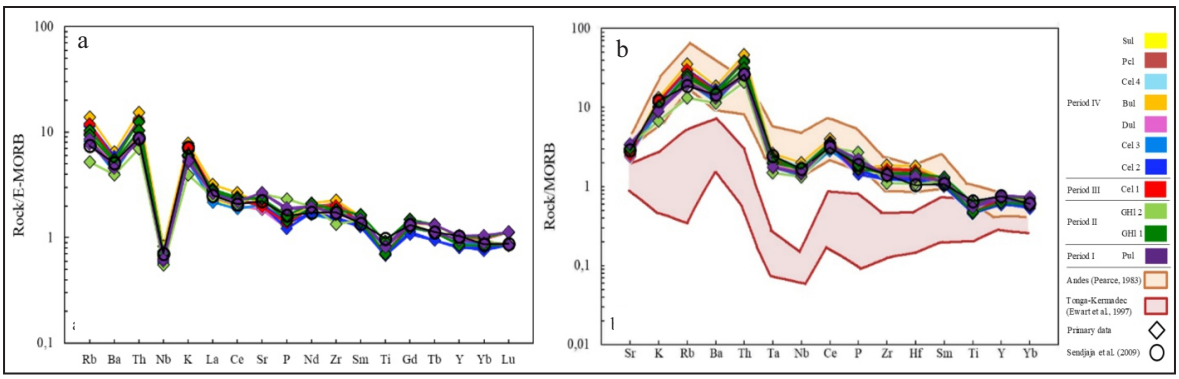


Figure 7. Spider diagrams of selected trace and rare-earth elements of The CVC. (a) Data normalized to Enriched MORB (E-MORB) (Sun and McDonough, 1989), and (b) data normalized to MORB (Pearce, 1983) compared with The Tonga-Kermadec Arc (Ewart *et al*., 1998) and Andes Arc (Pearce, 1983).

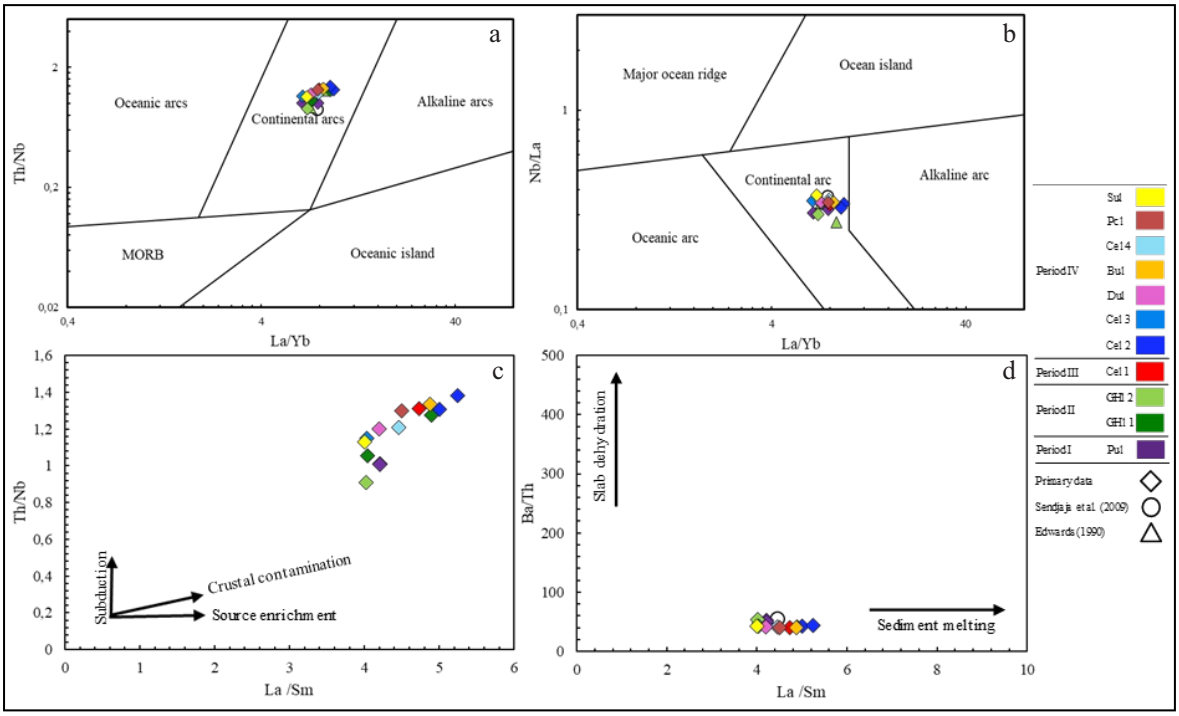


Figure 8. Tectonic discriminant diagrams, (a) Th/Nb vs. La/Yb, (b) Nb/La vs. La/Yb (Hollocher *et al*., 2012), (c) Th/Nb vs. La/Sm (Plank, 2005 in Barresi *et al*., 2015) and (d) Ba/Th vs. La/Sm (Labanieh *et al*., 2012).

by its tectonic setting, is distinguished by the ratio of Th/Nb vs. La/Sm (Plank, 2005 in Barresi *et al*., 2015; Figure 8d). Based on that ratio, during the earlier magmatism, the subduction-related enrichment is more dominant. Towards the later magmatism, the effects of crustal contamination became more pronounced.

The contribution of subducted components, such as (altered) oceanic crust or sediments, can strongly influence the magmatic source composition (Handley *et al*., 2007). The behaviour of trace elements during subduction is a major control on the geochemical signature of magmas. Some LILE are generally more mobile in aqueous fluids than REE or HFSE. Consequently, magmas derived from sources added by aqueous fluids typically display elevated LILE/REE or LILE/HFSE ratios compared to those influenced by partial melting of oceanic crust and subducted sediments (Özdemir and Güleç, 2014). Conversely, magmas affected by sediment melting often exhibit higher La/Sm ratios, although slab dehydration may

PUBLISHED IN IJOG

also occur concurrently (Labanieh *et al*., 2012). In the case of the CVC, all analysed lavas show consistently low Ba/Th and high La/Sm ratios. The low Ba/Th values (<170) resemble those of global subducting sediment (GLOSS), which are dominated by terrigenous material similar to the upper continental crust (Plank and Langmuir, 1998). This geochemical relationship suggests that source enrichment beneath the CVC primarily results from the subducted continental-derived sediments, rather than fluid additions from the altered oceanic crust (Figure 8d).

Discussion

Petrographic and geochemical analyses of the volcanic rocks from Ciremai indicate open-system behaviour in their magmatic processes. All samples exhibit porphyritic textures, where variations in crystal size reflect differences in magma cooling rates. Several microtextures further record dynamic magmatic conditions. Orthopyroxene phenocrysts rimmed by clinopyroxenes (Figure 4a) indicate unstable normal magmatic differentiation. The presence of gabbroic xenolith likely represents cumulate fragments derived from middle-lower crustal depths (Figure 4b). Significant changes in rock texture (hornblende andesite to basalt), mineral assemblages, and microtextures within its phenocrysts, such as in the last lava unit from Gegerhalang, indicate a significant basaltic magma influx and mixing within the magma chamber. The occurrence of antecrysts also suggests an ongoing interconnecting magmatic process from the previous periods (Figures 4d-e). The abundance of olivine in andesites and other microtextures, such as hornblende microphenocrysts with their disequilibrium textures, coarse sieved plagioclase, and skeletal olivine (Figures 4c, f-h), reflects chemical inequilibrium and magma reheating due to repeated basaltic injections within the magma chamber. Prolonged intermittent basaltic injection and reheating is also recorded as compositional zoning within plagioclase crystals. Partial dissolution in certain crystals (plagioclase and some pyroxenes) further evidences more intensive reheating and mixing episodes, resulting in pronounced sieving textures.

Based on the TAS diagram and magmatic affinity (Figure 5), the magma forming the CVC exhibits a clear calc-alkaline affinity. According to Wilson (1989), such calc-alkaline magmas are characteristic of convergent margins, typically reflecting subduction-related processes. A single trend of K_2O vs. SiO_2 suggests a progressive differentiation from a cogenetic magma source. Furthermore, the relatively uniform trace and rare-earth element compositions among the analysed volcanic rocks indicate derivation from a single, compositionally evolving magma chamber. Geochemical variations, particularly in the LILE/REE and LILE/HFSE, imply that the primary magma originated from partial melting of the subducted oceanic crust. Enrichment of certain elements suggests that the melting source was subsequently modified by the addition of subducted continental-derived sediments (Figures 7−8), showing a significant source-enrichment chemical signature. These characteristics collectively reflect a subduction environment where sediment contribution played a significant role in controlling magma composition beneath The CVC.

Geochemical analyses showed that the magmatic evolution of the CVC is primarily controlled by fractional crystallization of plagioclase (progressing from Ca-rich to Na-rich), along with pyroxene and/or olivine and Fe-Ti oxides, particularly in lower SiO_2 contents (Figure 6). However, the temporal variation of SiO_2 suggests recurrent influx and mixing of basaltic magma into a differentiated magma residing within the magma chamber. This process was most pronounced at the end of the Gegerhalang Volcano's activity, marked by a large injection and mixing of basaltic magma into a highly differentiated magma chamber. The resulting compositional and thermal disequilibrium likely destabilized the chamber, triggering a major eruption and the subsequent formation of the Gegerhalang Caldera. Minor

PUBLISHED IN IJOG

basaltic influxes and associated magma reheating at variable rates throughout later stages may have influenced the eruptive behaviour of the younger volcanic system in the CVC.

Conclusions

The activity of the Ciremai Volcanic Complex (CVC) is divided into four periods: Putri Volcano, Gegerhalang Volcano, Wurung Crater, and Ciremai Volcano (with its parasitic volcanoes). Patterns and abundances of trace and rare-earth elements suggest that the magma forming the CVC derived from the melting of subducted oceanic crust. Source enrichment and modification are predominantly due to the incorporation of a continental crust-derived sediment added to the mantle wedge. Based on microscopic petrographic analysis, volcanic rocks of the CVC are olivine basalts, basalts, pyroxene andesites, and hornblende andesites, all showing a porphyritic texture. Dominant phenocrysts are plagioclase, pyroxene, olivine, hornblende, and opaque minerals. The magmatic affinity of the CVC is mainly calc-alkaline, with an enrichment of Fe during the early magma generation. Variable petrographic characteristics and geochemical signatures suggest a temporal variation in the magmatic processes, driven predominantly by fractional crystallization, basaltic injection, and magma reheating, which suggest open-system magmatic dynamics. Geological records show that during the early activities in the CVC, continuous magmatic evolution from Putri to Gegerhalang ended with a major basaltic magma injection, destabilizing the evolved magma chamber. The injection and mixing previously explained, triggered an explosive Gegerhalang Caldera-forming eruption. Post-caldera magmatism of Wurung Crater, Ciremai, and its parasitic volcanoes are also affected by a prolonged basaltic influx and magma reheating throughout their evolutionary processes. Singular chemical evolutionary trends and homogeneous trace and rare-earth element compositions suggest similar processes in an interconnected open magmatic system throughout its history.

Acknowledgements

The authors acknowledge the PPMI FITB-ITB 2025 Programme from The Faculty of Earth Sciences and Technology for supporting this research.

References

Al Rasyid, G.I., 2016. *Geologi dan Petrogenesa daerah Gunung Ciremai dan sekitarnya, Kabupaten Majalengka, Kuningan, dan Cirebon*. Bachelor Thesis at Department of Geological Engineering, Faculty of Earth Sciences and Technology, Institut Teknologi Bandung.

Barresi, T., Nelson, J.L., Dostal, J., and Friedman, R., 2015. Evolution of the Hazelton arc near Terrace, British Columbia: Stratigraphic, geochronological, and geochemical constraints on a Late Triassic-Early Jurassic arc and Cu-Au porphyry belt. *Canadian Journal of Earth Sciences*, 52 (7), p.466-494. DOI: 10.1139/cjes-2014-0155.

Dempsey, S.R., 2013. *Geochemistry of volcanic rocks from the Sunda Arc*. Master's Thesis at Durham University.

Djuri, 1973. *Geologic map of the Ardjawinangun Quadrangle, Java, scale 1:100.000*, Directorate of Geology.

Edwards, C.M., 1990. *Petrogenesis of tholeiitic, calc-alkaline and alkaline volcanic rocks, Sunda Arc, Indonesia*. Dissertation at Royal Holloway University of London.

ESDM, 2021. *Tipe Gunung Api di Indonesia (A, B, dan C)*. https://magma.esdm.go.id/v1/edukasi/tipe-gunung-api-di-indonesia-a-b-dan-c

Ewart, A., Bryan, W.B., and Gill, J.B., 1973. Mineralogy and Geochemistry of the Younger Volcanic Islands of Tonga, S.W. Pacific. *Journal of Petrology*, 14 (3), p.429-465. DOI: 10.1093/petrology/14.3.429.

PUBLISHED IN IJOG

Ewart, A., Brothers, R.N., and Mateen, A., 1977. An outline of the geology and geochemistry, and the possible petrogenetic evolution of the volcanic rocks of the Tonga-Kermadec-New Zealand island arc. *Journal of Volcanology and Geothermal Research*, 2 (3), p.205-250. DOI: 10.1016/0377-0273(77)90001-4.

Ewart, A., Collerson, K.D., Regelous, M., Wendt, J.I., and Niu, Y., 1998. Geochemical Evolution within the Tonga-Kermadec-Lau Arc-Back-arc Systems: The Role of Varying Mantle Wedge Composition in Space and Time. *Journal of Petrology*, 39 (3), p.331-368. DOI: 10.1093/petroj/39.3.331

Global Volcanism Program, 2025. Ciremai (263170) *in* [Database] Volcanoes of the world (v. 5.3.2; 30 September 2025). Distributed by Smithsonian Institution, compiled by Venzke, E. DOI: 10.5479/si.GVP.VOTW5-2025.5.3.

Hall, R. and Sevastjanova, I., 2012. Australian crust in Indonesia, *Australian Journal of Earth Sciences*, 59 (6), p.827-844. DOI: 10.1080/08120099.2012.692335.

Hall, R., 2014. The origin of Sundaland. *Proceedings of Sundaland Resources Annual Convention*, p.17-18.

Hall, R., 2017. Southeast Asia: New Views of the Geology of the Malay Archipelago. *Annual Review of Earth and Planetary Sciences*, 45 (1), p.331-358. DOI: 10.1146/annurev-earth-063016-020633.

Handley, H.K., Macpherson, C.G., Davidson, J.P., Berlo, K., and Lowry, D., 2007. Constraining fluid and sediment contribution to subduction-related magmatism in Indonesia: Ijen Volcanic Complex, *Journal of Petrology,* 48 (6), p.1155-1183. DOI: 10.1093/petrology/egm013.

Hollocher, K., Robinson, P., Walsh, E., and Roberts, D., 2012. Geochemistry of amphibolite-facies volcanics and gabbros of the Storen Nappe in extensions west and southwest of Trondheim, western gneiss region, Norway: A key to correlations and paleotectonic settings. *American Journal of Science*, 312 (4), p. 357-416. DOI: 10.2475/04.2012.01.

Irvine, T.N. and Baragar, W.R.A., 1971. A Guide to the Chemical Classification of the Common Volcanic Rocks. *Canadian Journal of Earth Sciences*, 8 (5), p.523-548. DOI: 10.1139/e71-055.

Kadarsetia, E., 2013. Geokimia Batuan Gunung Api Ciremai, Jawa Barat. *Geologi dan Geokimia Batuan Gunung Api Ciremai, Jawa Barat*, p. 1-36.

Kusumadinata, K., 1971. *Gunung Tjiremai: Kumpulan data mentah hingga bulan April 1971*. Directorate of Geology, ESDM.

Labanieh, S., Chauvel, C., Germa, A., and Quidelleur, X., 2012. Martinique: a clear case for sediment melting and slab dehydration as a function of distance to the trench. *Journal of Petrology*, 53c (12), p.2441-2464. DOI: 10.1093/petrology/egs055.

Le Bas, M.J., Maitre, R.W.L., Streckeisen, A., Zanettin, B., and IUGS Subcommission on the Systematics of Igneous Rocks, 1986. A Chemical Classification of Volcanic Rocks Based on the Total Alkali-Silica Diagram. *Journal of Petrology*, 27 (3), p.745-750. DOI: 10.1093/petrology/27.3.745.

Miyashiro, A., 1975. Volcanic Rock Series and Tectonic Setting. *Annual Review of Earth and Planetary Sciences*, 3 (1), p.251-269. DOI: 10.1146/annurev.ea.03.050175.001343.

Özdemir, Y. and Güleç, N., 2014. Geological and geochemical evolution of the Quaternary Süphan Stratovolcano, Eastern Anatolia, Turkey: Evidence for the lithosphere-asthenosphere interaction in post-collisional volcanism. *Journal of Petrology*, 55 (1), p.37-62. DOI: 10.1093/petrology/egt060.

Padang, N.V., 1951. *Catalogue of the Active Volcanoes of the World, Including Solfatara Fields: Indonesia*, International Volcanological Association.

Pearce, J.A., 1983. Role of the sub-continental lithosphere in magma genesis at active continental margins. *In*: C.J. Hawkesworth and M.J. Norry (eds.), *Continental basalts and mantle xenoliths*. Shiva Publications, Nantwich, Cheshire, p.239-249.

PUBLISHED IN IJOG

Peccerillo, A. and Taylor, S. R., 1976. Geochemistry of Eocene calc-alkaline volcanic rocks from the Kastamonu area, Northern Turkey. *Contributions to Mineralogy and Petrology*, 58 (1), p.63-81. DOI: 10.1007/BF00384745.

Plank, T. and Langmuir, C.H., 1998. The chemical composition of subducting sediment and its consequences for the crust and mantle. *Chemical Geology*, 145, p.325-394.

Plank, T., 2005. Constraints from Thorium/Lanthanum on Sediment Recycling at Subduction Zones and the Evolution of the Continents. *Journal of Petrology*, 46 (5), p.921-944. DOI: 10.1093/petrology/egi005.

Renjith, M.L., 2014. Micro-textures in plagioclase from 1994-1995 eruption, Barren Island Volcano: Evidence of dynamic magma plumbing system in the Andaman subduction zone. *Geoscience Frontiers*, 5 (1), p.113-126. DOI: 10.1016/j.gsf.2013.03.006.

Rudnick, R L. and Gao, S., 2014. 4.1 - Composition of the Continental Crust. *In*: Holland, H.D. and Turekian, K.K. (eds.), *Treatise on Geochemistry* (second edition), Elsevier. DOI: 10.1016/B978-0-08-095975-7.00301-6.

Sendjaja, Y.A., Kimura, J.I.., and Sunardi, E., 2009. Across-arc geochemical variation of Quaternary lavas in West Java, Indonesia: Mass-balance elucidation using arc basalt simulator model. *Island Arc*, 18 (1), p.201-224. DOI: 10.1111/j.1440-1738.2008.00641.x.

Sendjaja, Y.A. and Kimura, J.I., 2010. Geochemical variation in Tertiary-Quaternary lavas of the West Java arc, Indonesia: Steady-state subduction over the past 10 million years. *Journal of Mineralogical and Petrological Sciences*, 105 (1), p.20-28. DOI: 10.2465/jmps.080930.

Situmorang, T., Hadisantono, R.D., and Asmoro, P., 1995. *Geologic map of Ciremai Volcano, West Java, scale 1:50.000*, Directorate of Volcanology, ESDM.

Stehn, C.H.E., 1940. Volcanic phenomena, East Indonesia. *Volcanological Survey Bulletin*, 5, p.87-94.

Streck, M.J., 2008. Mineral textures and zoning as evidence for open system processes. *Reviews in Mineralogy and Geochemistry*, 69 (1), p.1-28. DOI: 10.2138/rmg.2008.69.

Sun, S.S. and McDonough, W.F., 1989. Chemical and isotopic systematics of oceanic basalts: implications for mantle composition and processes. *Geological Society, London, Special Publication*s, 42 (1), p.313-345. DOI: 10.1144/GSL.SP.1989.042.01.19.

Tsuchiyama, A., 1986. Experimental study of olivine-melt reaction and its petrological implications. *Journal of Volcanology and Geothermal Research*, 29 (1-4), p.245-264. DOI: 10.1016/0377-0273(86)90047-8.

Vernon, R.H., 2018. *A Practical Guide to Rock Microstructure*, Cambridge University Press. DOI: 10.1017/9781108654609.

Williams, H., Turner, F.J., and Gilbert, C.M., 1982. *Petrography: An Introduction to the Study of Rocks in Thin Sections*, W.H. Freeman, San Francisco.

Wilson, M., 1989. *Igneous Petrogenesis: A Global Tectonic Approach*, Springer. DOI: 10.1007/978-1-4020-6788-4.

PUBLISHED IN IJOG